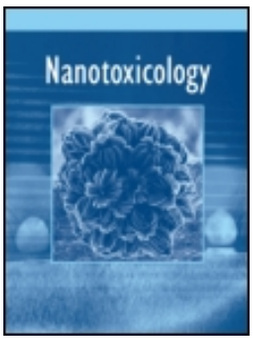

Nanotoxicology

ISSN: 1743-5390 (Print) 1743-5404 (Online) Journal homepage: https://www.tandfonline.com/loi/inan20

Comprehensive assessment of nephrotoxicity of intravenously administered sodium-oleate-coated ultra-small superparamagnetic iron oxide (USPIO) and titanium dioxide (TiO_2) nanoparticles in rats

Katarína Šebeková, Mária Dušinská, Kristína Simon Klenovics, Radana Kollárová, Peter Boor, Anton Kebis, Marta Staruchová, Barbora Vlková, Peter Celec, Július Hodosy, Ladislav Bačiak, Radka Tušková, Milan Beňo, Jana Tulinská, Jana Príbojová, Dagmar Bilaničová, Giulio Pojana, Antonio Marcomini & Katarína Volkovová

To cite this article: Katarína Šebeková, Mária Dušinská, Kristína Simon Klenovics, Radana Kollárová, Peter Boor, Anton Kebis, Marta Staruchová, Barbora Vlková, Peter Celec, Július Hodosy, Ladislav Bačiak, Radka Tušková, Milan Beňo, Jana Tulinská, Jana Príbojová, Dagmar Bilaničová, Giulio Pojana, Antonio Marcomini & Katarína Volkovová (2014) Comprehensive assessment of nephrotoxicity of intravenously administered sodium-oleate-coated ultra-small superparamagnetic iron oxide (USPIO) and titanium dioxide (TiO_2) nanoparticles in rats, Nanotoxicology, 8:2, 142-157, DOI: 10.3109/17435390.2012.763147

To link to this article: https://doi.org/10.3109/17435390.2012.763147

Nanotoxicology, March 2014; 8(2):142–157

ISSN: 1743-5390 print / 1743-5404 online
DOI: 10.3109/17435390.2012.763147

informa
healthcare

Comprehensive assessment of nephrotoxicity of intravenously administered sodium-oleate-coated ultra-small superparamagnetic iron oxide (USPIO) and titanium dioxide (TiO_2) nanoparticles in rats

Katarína Šebeková[1], Mária Dušinská[2], Kristína Simon Klenovics[3], Radana Kollárová[1], Peter Boor[4,1], Anton Kebis[5], Marta Staruchová[6], Barbora Vlková[1], Peter Celec[1], Július Hodosy[1], Ladislav Bačiak[7], Radka Tušková[7], Milan Beňo[6], Jana Tulinská[8], Jana Príbojová[9], Dagmar Bilaničová[10], Giulio Pojana[11], Antonio Marcomini[10], & Katarína Volkovová[6]

[1]Institute of Molecular Biomedicine, Medical Faculty, Comenius University, Bratislava, Slovakia, [2]NILU - Norwegian Institute for Air Research, Health Effects Laboratory, Kjeller, Norway, [3]Institute of Physiology, Medical Faculty, Comenius University, Bratislava, Slovakia, [4]Division of Nephrology and Institute of Pathology, RWTH University of Aachen, Aachen, Germany, [5]Laboratory of Organ Perfusion of Slovak Center of Organ Transplantation, Slovak Medical University, Bratislava, Slovakia, [6]Department of Experimental and Applied Genetics, Slovak Medical University, Bratislava, Slovakia, [7]Department of NMR Spectroscopy and Mass Spectroscopy, Faculty of Chemical and Food Technology, Slovak University of Technology, Bratislava, Slovakia, [8]Department of Immunology and Immunotoxicology, Slovak Medical University, Bratislava, Slovakia, [9]Department of Bioactive Substances in Foods, Slovak Medical University, Bratislava, Slovakia, [10]Department of Environmental Sciences, University "Ca' Foscari" of Venice, Venice, Italy and [11]Department of Philosophy and Cultural Heritage, University "Ca' Foscari" of Venice, Venice, Italy

Abstract

As a main excretory organ, kidney is predisposed to direct/indirect injury. We addressed the potential nephrotoxic effects following expositions of healthy rats to nanoparticle (NP) loads relevant to humans in a situation of 100% bioavailability. Up to 4 weeks after administration, a single iv bolus of oleate-coated ultra-small superparamagnetic iron oxide NPs (in dose of 0.1%, 1.0% and 10.0% of LD50) or TiO_2 NPs (1.0% of LD50) did not elicit decline in renal function, damage to proximal tubules, alterations in: renal histology or expression of pro-inflammatory/pro-fibrotic genes, markers of systemic or local renal micro-inflammation or oxidative damage. Antioxidant enzyme activities in renal cortex, mildly elevated at 24 h, completely restored at later time points. Data obtained by multifaceted approach enable the prediction of human nephrotoxicity during preclinical studies, and may serve as comparison for alternative testing strategies using *in vitro* and *in silico* methods essential for the NP-nephrotoxicity risk assessment.

Keywords: nanoparticles, renal function, oxidative stress, micro-inflammation, gene expression, renal histology

Introduction

Recent exploitation of nanotechnology is resulting in increased production of nanomaterials with broad application in different fields, including nanomedicine where humans are intentionally subjected to direct contact with engineered nanomaterials (ENMs). Translation of ENMs into clinical practice is developing in a rapid pace: nanoparticles (NPs) are being implemented to improve the effectiveness of both diagnostics (e.g. contrast agents for *in vivo* imaging, cells tracking) and therapy (e.g. coating of implants, bone replacement materials, coating or carriers of active substances to achieve better pharmacologic qualities and/or targeted drug delivery) (Pándics 2008).

Physicochemical and biological properties of nanomaterials may substantially differ from those of bulk material. Small size renders high surface reactivity and enables NPs cross biological barriers. These unique properties might also give rise to unexpected toxicities (Holsapple et al. 2005; Tetley 2007). The rapid progress in development and use of ENMs is not yet matched with toxicological investigations, and the growing use of nanomaterials in clinical practice requires the application of suitable strategies in human health risk assessment (Dusinska et al. 2009; Oberdorster 2010).

As a main excretory organ, kidney is predisposed as target to direct and/or indirect injury. High susceptibility to nephrotoxic injury stems from several factors of renal physiology: high renal blood flow renders kidney about 50 times higher rate of delivery of blood-born substances in comparison with the majority of other tissues. As a sequel of urinary concentrating process, the renal concentrations of certain solutes

Correspondence: Katarína Šebeková, Institute of Molecular BioMedicine, Medical Faculty, Comenius University, Sasinkova 4, 811 08 Bratislava, Slovakia. Tel: +421 2 59357 429. Fax: +421 2 59357 631; E-mail: kata.sebekova@gmail.com

(Received 15 September 2012; accepted 29 December 2012)

are several times higher than in tissues elsewhere in the body. High activity of renal metabolic processes and tubular transport require considerable oxygen supply; thus, except for oxygen deprivation and changes in blood flow, decrease in renal antioxidant enzyme activities or depletion of natural antioxidants may promote renal damage. The high capillary hydrostatic pressure and the largest endothelial surface per gram of tissue favour trapping of circulating substances in kidneys. Kidney may also be secondarily afflicted in presence of remote organ dysfunction. Pathologies frequently coexist because of organ cross talk, mediated via sympathetic signalling, circulating inflammatory mediators, systemically enhanced oxidative stress or other endogenous molecules released from injured tissue, activated phagocytes and/or platelets (Aurelie & Touyz 2011; Cruz et al. 2012; Koomans et al. 2004; Rosner et al. 2012; Singbartl 2011).

Although kidney has been identified as a potential main target of NP toxicity (Pujalte et al. 2011; Stern & McNeil 2008), studies on nephrotoxicity of NPs are scarce, and diverse methodological approaches yield different results. *In vivo* studies referring to oral expositions via gavage (with uncertain bioavailability of NPs) consistently report dose-dependent effects of metal-containing NPs (ZnO, nanocopper, TiO_2) with overt nephrotoxicity manifested at supramaximal dosages (Fadda et al. 2012; Lei et al. 2008; Liao & Liu 2012; Wang et al. 2007; Yan et al. 2012; Zhang et al. 2010). On the other hand, no signs of nephrotoxicity were revealed after single iv administration of ultra-small superparamagnetic iron oxide (USPIO) or TiO_2 NPs to rats in lower-than-supramaximal doses in acute and subchronic settings (Fabian et al. 2008; Jain et al. 2008; van Ravenzwaay et al. 2009). *In vitro* studies on human glomerular mesangial (IP15) and proximal epithelial (HK-2) cell lines indicated nephrotoxic potential of ZnO and CdS, but not TiO_2, NPs (Pujalte et al. 2011).

Studies comprehensively addressing the potential nephrotoxic effects following expositions of healthy rats to NP loads relevant to humans in a situation of 100% bioavailability are missing, despite the knowledge that only testing levels relevant to human exposure, e.g. avoiding overload conditions, enable to evaluate the true health risk of these materials (Holsapple et al. 2005). Herein we studied the nephrotoxicity of iv administered oleate-coated USPIO and TiO_2 NPs 24 h, 1, 2 and 4 weeks after their administration in a single dose, and compared with the findings in placebo-administered rats. Iron oxide NPs were used owing to their wide application in modern medicine and pharmacology, among others, as contrast enhancers in nuclear magnetic resonance (NMR) imaging (MRI), for targeted drug delivery, controlled drug release, cancer therapy by hyperthermia, as well as labels in cell tracking (Duguet et al. 2006; Majewski & Thierry 2007), while oleate coating was selected for testing, since oleate-coated USPIO NPs display an excellent biocompatibility, magnetic properties and dispersion in aqueous solutions (Sun et al. 2007). Oleate-coated USPIO NPs were administered in a single bolus in three dosages (0.1%, 1.0% and 10.0% of estimated LD50); thus, the highest administered dose of iron (47.2 μmol Fe/kg) exceeded the diagnostic dose for MRI in humans (10–15 μmol Fe/kg) (Laniado & Chachuat 1995) 3–5-fold. Lower doses were tested owing to the fact that they may mimic the exposure with uncertain bioavailability, such as oral or by inhalation, as well as since the yet unpublished data from some cell culture experiments, carried out within the NanoTEST project (www.nanotest-fp7.eu) by other groups, suggested occasional inverse toxicity to applied NP concentrations. Insoluble non-toxic metallic material – nanosized TiO_2 – was used as negative reference, taking into consideration that iv administration of TiO_2 NPs in dose 10-fold higher than that used in our study neither induced nephrotoxic effects, nor evoked systemic oxidative stress or micro-inflammation (Fabian et al. 2008), as well as its bulk production and wide application in various fields of science and technologies, including cosmetics (sunscreens and anti-ageing agents), food industry (colour additives) (Park et al. 2006; Wang et al. 2007) and medicine – particularly virology, microbiology and oncology (Ismagilov et al. 2009). Anticipating that a human exposure to TiO_2 NPs is rather low, herein the rats were exposed to 1.0% of estimated LD50, e.g. 0.592 mg TiO_2/kg.

Due to high functional reserve of the kidney, routinely used blood and urine markers of renal function may remain within the normal range even while 65–75% of kidney function is lost; thus, they are insensitive and non-specific indicators of renal injury (Han et al. 2002; Star 1998). Alterations in renal histomorphology and gene expression may precede a decline in renal function (Boor et al. 2009). To objectivise the nephrotoxic potential of administered NPs, we employed comprehensive approach: standard tests of renal function, renal histology, pro-fibrotic and pro-inflammatory genes expression in renal tissue, as well as determination of different non-standard markers, such as urinary excretion of kidney injury molecule-1 (KIM-1, recently accepted by the European Medicines Agency – EMEA and US Food and Drug Administration – FDA as an early diagnostic biomarker of drug-induced acute kidney tubular alterations in rat toxicology studies) (Vaidya et al. 2010). Since experimental studies suggest that induction of oxidative stress might be one of the common denominators of toxic potential of metal oxide NPs (Kim et al. 2012; Zhang et al. 2010), from among the potential uremic toxins (i.e. substances accumulating in proportion to the decline of renal function) (Vanholder et al. 2003) we selected those being concurrently also markers of oxidative damage to proteins or lipids. Since NPs deposited in one organ may access blood or lymph vessels and target other organs (Tetley 2007), we focussed simultaneously on both, systemic and local alterations, e.g. circulating biomarkers and their accumulation in renal tissue.

Methods

The study was conducted according to the guidelines for experimental studies using laboratory animals (86/609/EEC), after the approval by the Institutional Ethics Board for Experimental Animals (SMU, Bratislava, Slovakia), and the State Veterinary and Food Control Agency in Bratislava (Slovakia).

Characterisation of NPs

NPs used in this study are commercially available and were provided with physicochemical characterisation by the provider (Table I), while some further characteristics (e.g. the size distribution by dynamic light scattering - NICOMP 370 submicron particle sizer, DSS, CA, USA; pH analyses) were performed on request within the NanoTEST Consortium at University of Venice. Detailed physicochemical characteristics of employed NPs were published previously (Kenzaoui et al. 2012; Magdolenova et al. 2011). In brief, TiO_2 NPs (P25 obtained from Evonik Degussa GmbH., Essen, Germany; typically reported as a mixture of anatase and rutile crystallites in a ratio of 70:30 or 80:20) (Ohtani et al. 2010) were provided by Joint Research Center (Ispra, Italy). They were suspended in physiological solution containing 10% v/v of rat serum (Sigma), pH = 7.5, and sonicated (Dynatech Artek 300, Manassas, VA, USA) for 15 min at 150 W. In this suspension, the TiO_2 NPs displayed bimodal size distribution, with peaks at 84 ± 8 (61% of NPs) and 213 ± 15 nm. Sodium oleate (7% v/v)-coated USPIO NPs were purchased from PlasmaChem GmbH (Berlin, Germany). After heating to 38°C, the required volume was added to the physiological solution, and homogenised by shaking. In this solution with pH of 6.0, NPs displayed bimodal size distribution, peaking at 31 ± 4 (88% of NPs) and 122 ± 3 nm.

Estimation of median lethal dose (LD50) of NPs administered by a single iv injection

Forty-one female outbred Wistar rats (age: 8 weeks, weight: 205.5 ± 8.5 g) were used. Rats were housed at a rate of 2 animals per cage, under constant room temperature and humidity, 12 h/12 h light cycles (inversed to daylight), with *ad libitum* access to tap water and standard rat chow (SP1, Top Dovo, Horné Dubové, Slovakia). After adaptation period, NPs were administered iv, under xylazine anaesthesia. The study was performed according to OECD 425 guidelines (OECD 2000), and an estimate of the LD50 and a confidence interval were calculated using the AOT425StatPgm software (http://www.epa.gov/oppfead1/harmonization/), as described in detail in Volkovova et al. (2013).

Nephrotoxicity of NPs administered in a single iv injection

Sample size calculation

Sample size was calculated using available analytical data from our previous experiments on rats of corresponding strain and age. With 95% two-sided confidence interval and power of 80%, the calculated number to detect 2-fold increase was 4–7 rats per group, depending on the parameter used. The experiment was conducted using eight animals/group.

Experiment

The study was performed using 160 female Wistar rats (9–10 weeks old, weight 220 ± 22 g). Rats were housed under same conditions as given above. After adaptation period, rats were randomised into 5 groups (n = 32 rats, each group). TiO_2 NPs were administered in a dose of 1.0% of estimated LD50, corresponding to 0.592 mg/kg. Oleate-coated USPIO NPs were administered in three dosages (0.1%, 1.0% and 10.0% of estimated LD50), corresponding to 0.0364 mg Fe_3O_4/kg, 0.364 mg/kg and 3.64 mg/kg, respectively. Test substances were administered iv into the tail vein in dose of 0.5 µl/g body weight, under ketamine/xylazine anesthesia. Control group (CTRL) received vehicle (10% v/v rat serum in 0.9% NaCl). Rats were closely followed for 3 h after administration of test substances, and thereafter they were returned into the cages. After the single iv injection, 8 animals from each group were subsequently sacrificed 24 h, 1 week, 2 weeks or 4 weeks later.

During the study period, rats were weighed weekly, and food consumption was measured three times a week.

Systolic blood pressure (tail plethysmography in conscious rats, 2 days before sacrifice) was measured only in the rats sacrificed 4 weeks after administration of NPs (due to technical reasons).

Before sacrifice, animals were placed for 24 h in metabolic cages for stool-free urine collection (except for animals sacrificed after 24 h, which were held in metabolic cages for 15.5 h). Collected stool was weighed. Before sacrifice, animals were not subjected to fasting. At sacrifice, blood from abdominal aorta was collected into Li-heparin, K_2EDTA tubes, and tubes without anticoagulant, in the same manner from concurrent control and treatment groups of animals. Collection and pre-analytical processing were carried out in a way to minimise time-related biases.

Urinary analyses

Urine pH and volume were measured, and a dipstick method was used for semiquantitative determination of proteins, ketone bodies, urobilinogen, bilirubin, blood and glucose. Urines were analysed for creatinine, urea, sodium, potassium, calcium, iron and phosphate concentration (Vitros 250 analyzer, J&J, Rochester, NY, USA). Proteinuria was determined by a pyrogallol red method. Aliquots of urines were stored at −80°C for determination of KIM-1 (ELISA, USCN Life Sciences, Wuhan, China). Proteinuria and KIM-1 excretion are given as a ratio to urinary creatinine. Fractional excretion of sodium, potassium, calcium, iron and phosphate were calculated.

Blood chemistry

Blood count was determined using Sysmex K-20 analyzer (TOA Medical Electronics, Kobe, Japan) equipped with software for determination of rat blood counts. Heparinised plasma was used for standard biochemical (glucose, creatinine, urea, lipid profile, albumin, minerals, electrolytes, liver enzyme activities, Vitros 250 analyzer, J&J, Rochester, NY, USA) and all special analyses, except for that of rat-specific highly sensitive C-reactive protein (hsCRP) and asymmetric dimethylarginine (ADMA) determination, which were carried out in sera. Non-standard blood chemistry was determined from aliquots of plasma or serum stored at –80°C.

Rat-specific insulin and hsCRP (both from Biovendor, Modrice, Czech Republic), rat-specific ADMA and carbonyl proteins (both Immundiagnostik, Bernheim, Germany) and N^{ε}-(carboxymethyl)lysine (CML, MicroCoat Biotechnologie

Table I. Summary of primary physical and chemical properties of TiO_2 and oleate-coated ultra-small superparamagnetic iron oxide (USPIO) nanoparticles (NPs).

Primary physicochemical characteristics	TiO_2 NPs	USPIO NPs
Phase	White ultra-fine powder	Water dispersion
Shape of particles	Irregular/ellipsoidal	Oblong
Particle size (nm)	15–60	9 × 7
Crystal structure	Anatase/Rutile*	Spinel (octahedral)
Surface area (m^2/g)	61	NA
Pore volume (ml/g)	0.13	NA
Zeta-potential at pH 7 (mV)	–30.2	–31.9
Chemical composition of particles	Ti, O	Fe, O
Purity of particles	>99%	>99%
Surface chemistry	Uncoated	Oleate micelle coated
Impurities of concern	Co (920 ppm) Fe (16 ppm)	Free oleate (960 ppm) Na (26 ppm) Ca (1.3 ppm) K (730 ppm)

*Typically reported as a mixture of anatase and rutile crystallites in a ratio of 70:30 or 80:20 (Ohtani et al. 2010).

GmbH, Bernried, Germany, after pretreatment with proteinase K) were determined by ELISA methods according to manufacturers' instructions. advanced glyaction end products (AGE)-associated fluorescence of plasma was determined according to (Munch et al. (1997), and advanced oxidation protein products (AOPPs) according to (Witko-Sarsat et al. (1996). CML, AOPP, AGE-associated fluorescence and protein carbonyl levels were corrected for plasma albumin concentration.

Kidneys

Kidneys were removed, weighed, dissected and fixed (formaldehyde, Carnoy's solution) for histomorphological and immunohistochemical analyses, and a part of the cortex was removed and stored immediately in liquid nitrogen for subsequent DNA extraction. For determination of oxidative status parameters, aliquots of kidney cortex were sampled into ice-chilled tubes with phosphate-buffered saline (PBS), and kept frozen (–70°C) until processing.

Homogenates of renal cortex tissue in PBS, 10% (w/v), were prepared using Ultra-Turrax (IKA Works GmbH & Co. KG, Staufen, Germany) homogeniser (2 × 10 sec with 15 sec cooling interval) and centrifuged at 600 g for 10 min at 4°C to obtain the supernatant fraction.

Oxidative status parameters in renal cortex

Activities of glutathione peroxidase (GPX) (Paglia & Valentine 1967) and glutathione S-transferase (GST) (Habig et al. 1974) were determined by kinetic method. Catalase (CAT) activity was measured spectrophotometrically (Cavarocchi et al. 1986). The activity of superoxide dismutase (SOD) was estimated employing a commercial kit (Randox Lab. Ltd, Crumlin, UK). Enzyme activities were expressed per 1 mg of protein determined in kidney cortex homogenates (Bradford 1976).

Malondialdehyde (MDA)–thiobarbituric acid adduct levels were determined employing high performance liquid chromatography (HPLC) method with fluorimetric detection (λ_{ex} = 532 nm; λ_{em} = 553 nm) according to the original method (Wong et al. 1987), as modified by Koska et al. (Koska et al. 1999), and in renal cortex expressed per 1 g of tissue.

Ferric reducing ability of tissue homogenates was measured according to the original protocol of Benzie and Strain (Benzie & Strain 1996), as modified by (Celec et al. (2012).

Content of AOPPs (Witko-Sarsat et al. 1996) in kidney cortex homogenates was expressed per gram protein (Bradford 1976).

Gene expression

Total RNA was isolated from the renal cortex using the TRI Reagent (MRC, Cambridge, UK). Quantity and purity of the isolates were measured spectrophotometrically using Biophotometer (Eppendorf, Hamburg, Germany). The expressions of TGF-β1, collagen I and TNF-α were analysed using the QuantiFast SYBR Green RT-PCR Kit (Qiagen, Hilden, Germany) on a Mastercycler ep realplex (Eppendof, Hamburg, Germany) with cyclophilin A as the housekeeping gene. The comparative Ct method was used to calculate the relative expression. Primers used for real-time polymerase chain reaction are given in Table II.

Renal histology and immunohistochemistry

Renal tissue was immersion-fixed in methyl Carnoy's or formalin solution directly after sacrifice and embedded in paraffin (Boor et al. 2007; Boor et al. 2011). Thin sections (<2 μm) were stained with periodic acid Schiff (PAS) for assessment of renal histopathology and with Turnbull Blue (staining for Fe^{2+} and Fe^{3+}) or Berlin Blue (staining for Fe^{3+} only) according to standard protocols for assessment of possible renal accumulation of administered oleate-coated USPIO NPs. In Sirius red staining for each animal the extent of renal cortex with fibrosis (positive birefringence) was scored individually in renal cortex and outer medulla as follows: 0 – up to 5%, 1 – 6–25%, 2 – 26–50%, 3 – 51–75%, 4 – 76–100%. Collagen type I was stained using the indirect immunoperoxidase procedure as described previously (Boor et al. 2007; Boor et al. 2011). Goat polyclonal antibody to human collagen type I cross reactive with rat collagen I (dilution 1:500, Southern Biotechnology Associates, Birmingham, AL, USA), and biotinylated and affinity-purified secondary antibody (Vector, Burlingame, CA, USA) was used. Computer-based morphometric

Table II. Primers for gene expression analysis using real-time polymerase chain reaction used in this study (all 5′-3′).

Gene	Forward primer	Reverse primer
Ppia	Gtctcttttcgccgcttgct	Tctgctgtctttggaactttgtctg
Col1a1	Caacctcaagaagtccctgc	Acaagcgtgctgtaggtgaa
Tgfb1	Gaaggacctgggttggaagt	Tactgtgtgtccaggctcca
Tnfa	Atccgagatgtggaactggc	Tcagtagacagaagagcgtggtg

ppia, peptidylprolyl isomerase A (cyclophilin A); col1a1, collagen type I α1 chain; tgfb, transforming growth factor-β_1; tnfa, transforming growth factor-α.

analyses were used to analyse the cortical and outer medullary area positively stained for collagen type I, as described previously (Boor et al. 2007; Boor et al. 2011). All slides were analysed in a blinded fashion by an experienced nephropathologist.

Magnetic resonance imaging

NMR analysis of tissue T2 relaxation times was employed to confirm the potential iron deposition within the kidney, since superparamagnetic iron NPs exert strong effect on adjacent structures measurable as relaxation time T2 and T2* (two-dimensional relaxation) shortening. Formaldehyde-fixed kidneys (before embedding into paraffin) harvested 24 h after the administration of the vehicle or 10% of LD50 USPIO NPs were studied, while the corresponding livers (main target organ of Fe_3O_4 NPs) (Wang et al. 2010) served as positive controls. Organs from four randomly selected animals from each group were evaluated.

All experiments were performed on 4.7 T/210 mm horizontal magnet and DD2 console (Agilent, Yarton, UK) equipped with 12 cm shielded gradients with a maximum gradient strength of 400 mT/m. A quadrature transmit/receive birdcage volume coil (Rapid Biomed, Rimpar, GE) with an internal diameter of 72 mm was used for multiecho multislice spin echo experiments. Six to eight transversal slices with a thickness of 2 mm were selected to cover whole kidney. Seven to nine transversal slices were selected in the liver. Six echo times (TE = 9, 18, 27, 36, 45, 54 msec) were used for subsequent T2 calculation. Repetition time of 1000 msec with 10 averages resulted in the overall acquisition time of ~10 min. The acquired matrix size was 128 × 64 and field of view = 20 × 20 mm (30 × 20 mm for liver).

MRI data processing

Data were zero filled to 512 × 512 matrix size and Gaussian filter in time domain (gf = 0.00042, gfs = 0.00064 in readout direction, gf = 0.005508, gfs = 0.008359 in phase encoding direction) was applied for noise reduction. Regions of interest (ROIs) in kidney cortex were manually selected on each image slice (Figure 1, left). In the case of liver, on each slice the whole parenchyma excluding main ducts and vessels was selected (Figure 1, right).

Using Origin 7.0 software, the mean signal intensities of selected ROIs were plotted against the TE values and fitted simultaneously for all slices originated from the same sample by mono-exponential function by a least-square method algorithm. Thus, for each kidney or liver the mean T2 value ± SD was obtained. The standard T2 fitting function was modified for signal decay convergence to mean noise level represented by parameter I_{noise} in the function bellow:

$$I(TE) = I_0 * \exp(-TE / T2) + I_{noise}$$

I(TE) = signal intensity at the echo time TE; I_0 = signal intensity at zero echo time; I_{noise} = signal intensity of the mean noise level; TE = echo time; T2 = T2 relaxation time.

Statistical analyses

Data are given as mean (SD). Multiple groups were compared using Kruskal–Wallis test, with, if appropriate, *post hoc* exact Mann–Whitney *U*-test (two-sided) with Bonferroni correction for target alpha. Two-sided unpaired *t*-test was used to evaluate the MRI data. Categorical data were

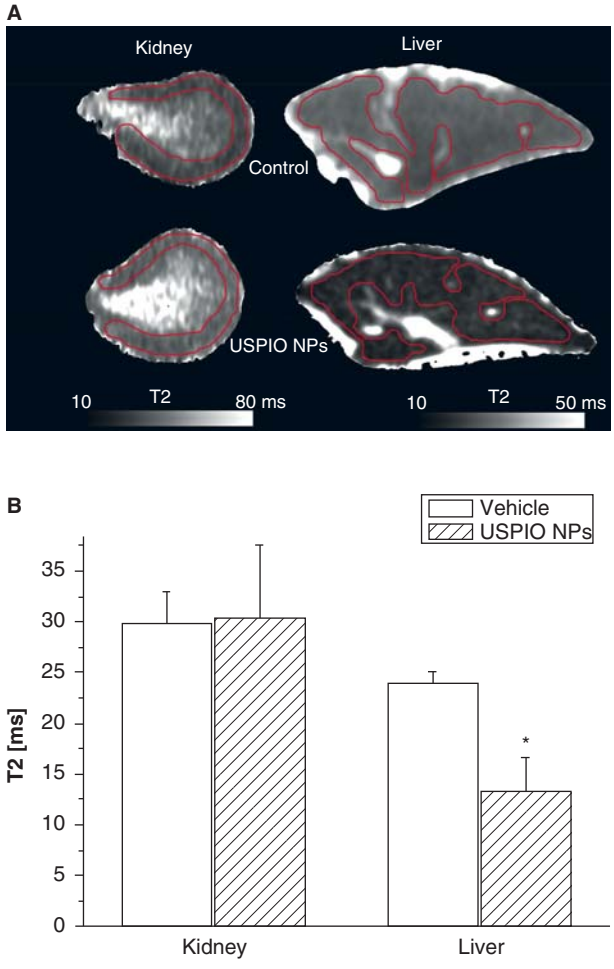

Figure 1. *Ex vivo* assessment of USPIO NPs deposition in kidney and liver tissue by magnetic resonance imaging 24 h after administration of the vehicle or oleate-coated USPIO NPs in dose corresponding to 10.0% of LD50 to healthy rats. (A) Representative T2 maps of kidney and liver, left and right, respectively. Upper row: organs of control animal, lower row: kidney and liver from rat administered oleate-coated USPIO NPs in a single dose of 3.64 mg Fe_3O_4/kg. Selected regions of interest (ROIs, delineated in red) in kidney cortex and liver parenchyma were used for T2 calculation. Being magnetic, USPIO NPs disrupt the magnetic signals in the MR scanner; thus, their deposits appear as dark areas. These diffuse hypointense areas can be clearly seen in whole liver parenchyma, however not in kidney. Note different scales used for kidneys and livers. (B) T2 relaxation times determined *ex vivo* in kidney cortices and livers. Control group: kidney: $n = 4$, liver: $n = 4$. USPIO NPs loaded group: kidney: $n = 4$, liver: $n = 3$. Data are given as mean ± SD. *: $p < 0.005$.

evaluated using chi-square. $p < 0.05$ was considered significant. SPSS v. 16 statistical program was used.

Results

Estimation of median lethal dose (LD50) of NPs administered by a single iv injection

The LD50 of TiO_2 NPs was calculated as 59.22 mg/kg, with confidence interval from 55 to 70 mg/kg. The LD50 of oleate-coated USPIO NPs was 36.42 mg/kg, with confidence interval (0–20,000 mg/kg). The latter experiment was finished via the software, since at a dose of 44 mg/kg one animal survived and two died; while at that of 35 mg/kg, one animal survived and one died. Experimental modelling indicated that including additional animals would not improve the outcome significantly.

Deposition of oleate-coated USPIO NPs in kidney measured by MR

Since iron oxide is magnetic, they disturb the local magnetic field in the tissue. The iron-containing NPs cause a dephasing of the nearby spins of water, thereby decreasing the signal intensity on a T2*-weighted images. Thus, the accumulation of NPs is indirectly recognised as decreased signal intensity in the MRI images. Twenty-four hours after administration of NPs, the density of MRI images of the kidneys of the vehicle-administered control animal and that of oleate-coated USPIO NPs loaded was similar (Figure 1A), indicating lack of MRI-detectable USPIO NPs deposition. Mean T2 relaxation time was calculated from ROIs (illustrated by red demarcation in Figure 1A) in each sample. As shown in Figure 1B, no significant difference in T2 value of kidney cortex was observed between control and oleate-coated USPIO NP-loaded groups ($p > 0.86$), even if evaluated by a standard T2 spectroscopic relaxometry protocol ($p > 0.87$; spin echo Tr = 5 sec, TE = 5, 10, 20, 40, 80, 160 msec; data not given). However, in contrast to MR image of the kidney, diffuse hypointense area resulting from USPIO NP deposits can be clearly seen in whole liver parenchyma (Figure 1A), indicating that liver is the main target organ of USPIO NPs. Signal loss in one liver sample in all echo times, probably due to strong T2* effect of huge oleate-coated USPIO NP deposits, precluded inclusion of this sample into the evaluation; thus, data obtained only from three oleate-coated USPIO NP-administered animals were considered. However, T2 value of liver was significantly lower in oleate-coated USPIO NP-administered group if compared with the controls ($p = 0.005$, Figure 1B).

Effects of administration of NP on renal function

At sacrifice, kidney weight (Supplementary Table Ia and Ib) or kidney-to-body weight ratio (Figure 2A) did not differ significantly between the groups in either time interval.

The NP-administered groups did not differ significantly from the controls in either time interval in plasma creatinine and urea levels, diuresis or creatinine clearance – regardless whether corrected for body weight (Supplementary Table IIa and IIb) or per kidney weight (data not given). Administration of NPs did not affect significantly the urinary pH except for the animals sacrificed 2 weeks after administration of NPs, when the groups receiving TiO_2 NPs and 1.0% of LD50 of oleate-coated USPIO NPs presented significantly more acidic urines if compared with the controls (Supplementary Table IIa and IIb). Dipstick analyses did not indicate significant differences in urinary haemoglobin, ketone bodies, bilirubin and urobilinogen between the groups in either time interval (data not given).

Determinations of protein excretion rate (Figure 2B), or renal excretion of KIM-1, a marker of the damage to proximal tubules (Figure 2C), did not reveal any significant difference among the groups in either time interval.

No significant differences in plasma potassium and phosphate levels were revealed between the groups at either time point of investigation (Supplementary Table IIa and IIb). Rats sacrificed 1 week after administration of 1.0% and 10.0% of LD50 of oleate-coated USPIO presented higher concentration of plasma sodium in comparison with the control animals, while elevation of calcium and magnesium was revealed only in the animals injected with the highest dose (Supplementary Table IIa and IIb). However, these significances in electrolyte and mineral concentrations were detected within the normal range of these parameters. Urinary excretion (data not given) and the fractional excretion of the mentioned electrolytes and minerals did not differ between the groups in either time interval (Supplementary Table IIa and IIb).

Administration of NPs did not affect significantly the plasma levels of ADMA (Supplementary Table IIIa and IIIb).

Effects of administration of NPs on markers of systemic inflammation and oxidative status

We did not observe any significant change in the markers of inflammation: white blood cell counts (Supplementary Table Ia and Ib), hsCRP levels (an acute phase reactant with half-life of about 2 h) (Figure 3A) and AOPPs (markers of neutrophiles activation), (Figure 3B). Circulating levels of modified proteins – fluorescent advanced glycation end products, protein carbonyls, (Supplementary Table IIIa and IIIb) and carboxymethyllysine (Figure 4A) – did not display significant between-group differences in either investigated time interval.

Biomarkers of oxidative status, inflammation and fibrosis in renal cortex homogenates

Oxidative damage markers

Administration of NPs did not affect the accumulation of AOPPs (Figure 3C) or MDA in renal cortex at either time interval (Figure 4B).

Markers of antioxidative defense

Twenty-four hours after the administration of NPs a rise in SOD activity in renal cortex was observed in the rats administered 1.0% of LD50 oleate-coated USPIO (Figure 4C), and a rise in GST activity in those administered TiO_2 NPs (Figure 4D) if compared with the controls. Activities of these enzymes showed no significant difference among the groups in other three time intervals (Figure 4C–D). On the other hand, the groups administered NPs did not differ significantly from the controls in the activity of GPX or CAT, and the ferric reducing ability of renal cortex tissue at either time interval (Supplementary Table IIIa and IIIb).

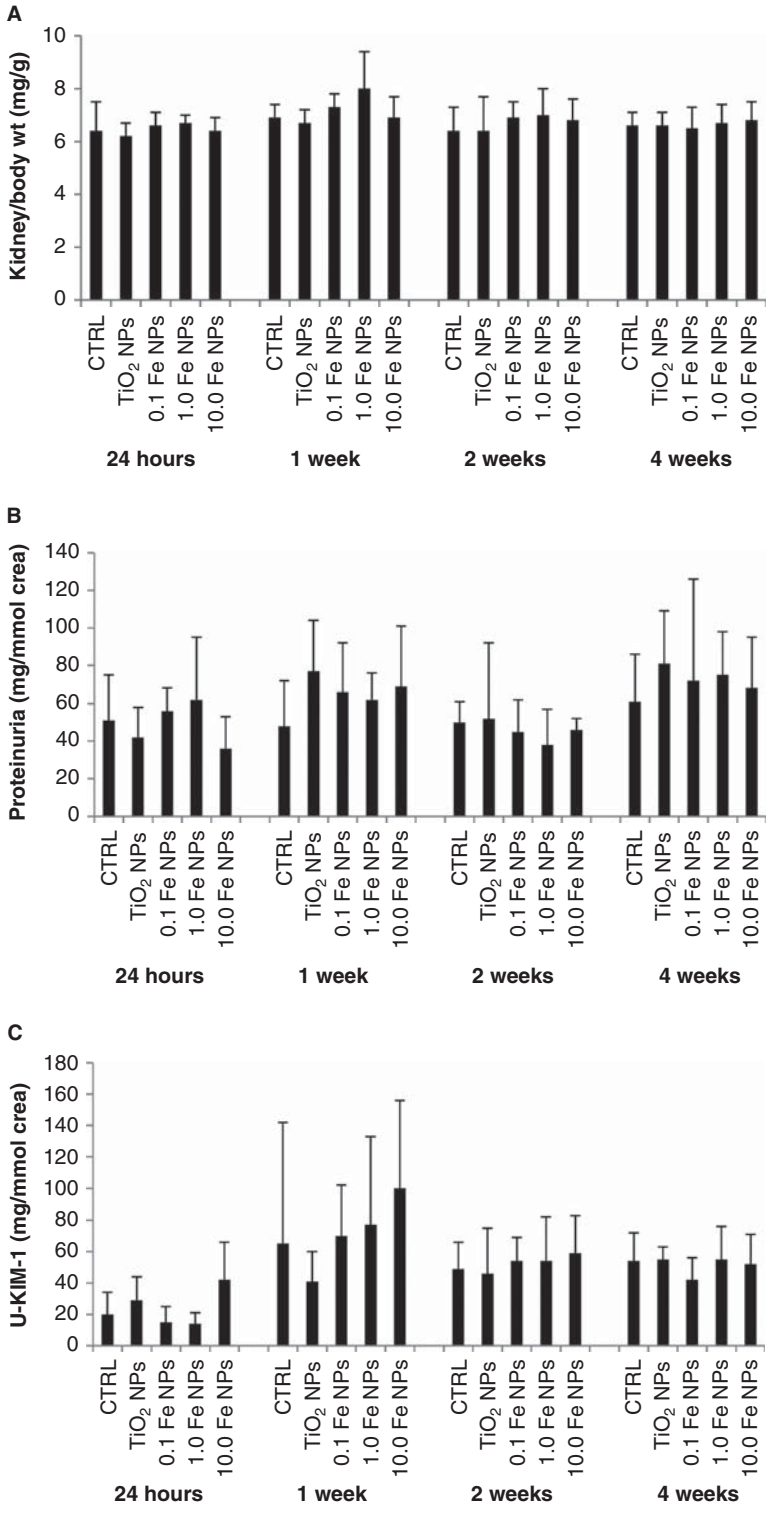

Figure 2. Parameters of renal function after single iv administration of NPs to healthy rats. (A) kidney-to-body weight (wt) ratio; (B) protein excretion rate corrected for urinary creatinine (crea), and (C) urinary excretion of kidney injury molecule-1 (KIM-1, a marker of damage to proximal tubules) corrected for crea of placebo (CTRL)-administered rats; those injected with iv bolus of TiO_2 NPs in dose of 1.0% of LD50; and oleate-coated USPIO NPs administered in doses corresponding to 0.1%, 1.0% and 10.0% of LD50, respectively. Rats were sacrificed 24 h, 1, 2 and 4 weeks after single administered dose. Each group represents mean (SD) from 6 to 8 animals.

Expression of pro-fibrotic genes

We revealed no significant differences in the expression of TGF-β_1- or that of collagen I-mRNA among the groups in either time interval (Supplementary Table IIIa and IIIb).

Expression of pro-inflammatory TNF-α gene

Administration of NPs did not elicit significant change in the expression of TNF-α-mRNA in either time interval (Supplementary Table IIIa and IIIb).

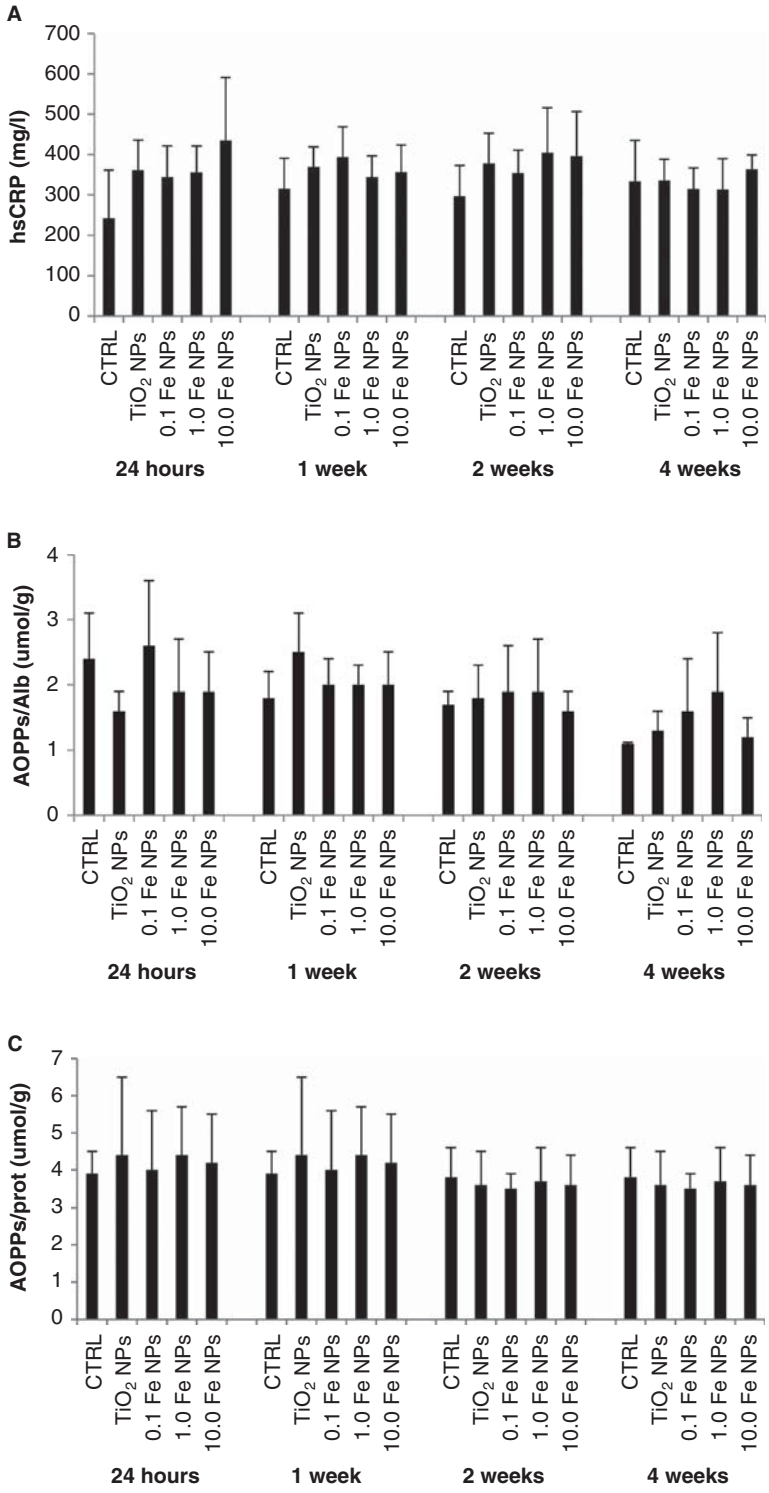

Figure 3. Markers of systemic inflammation or local inflammation in renal cortex homogenates in healthy rats after iv administration of single dose of NPs. (A) Plasma highly sensitive C-reactive protein (hsCRP, acute phase reactant, marker of micro-inflammation, hsCRP); (B) plasma content of advanced oxidation protein products (AOPPs) corrected for albumin (alb) (a marker of protein oxidation via myeloperoxidase reaction); and (C) content of AOPPs in renal cortex homogenates corrected for 1 g protein (prot) at sacrifice. CTRL: placebo-administered rats; TiO_2 NPs: rats injected with iv bolus of TiO_2 NPs in dose of 1.0% of LD50; Fe NPs: oleate-coated USPIO NPs administered in doses corresponding to 0.1%, 1.0% and 10.0% of LD50, respectively. Rats were sacrificed 24 h, 1, 2 and 4 weeks after single administered dose. Each group represents mean (SD) from 6 to 8 animals.

Renal histology and immunohistochemistry

Histomorphological evaluation of the kidneys did not reveal alterations which might have preceded a decline in renal function: at each time point, all animals showed normal renal structure without any obvious pathological changes (Figure 5). In particular, no signs of tubular toxicity (e.g. necrosis, apoptosis, vacuolisation, atrophy, increased proliferation, oedema) were observed. Glomeruli, renal macro- and micro-vasculature and interstitium showed no pathology as well (Figure 5). In accordance to MRI analyses,

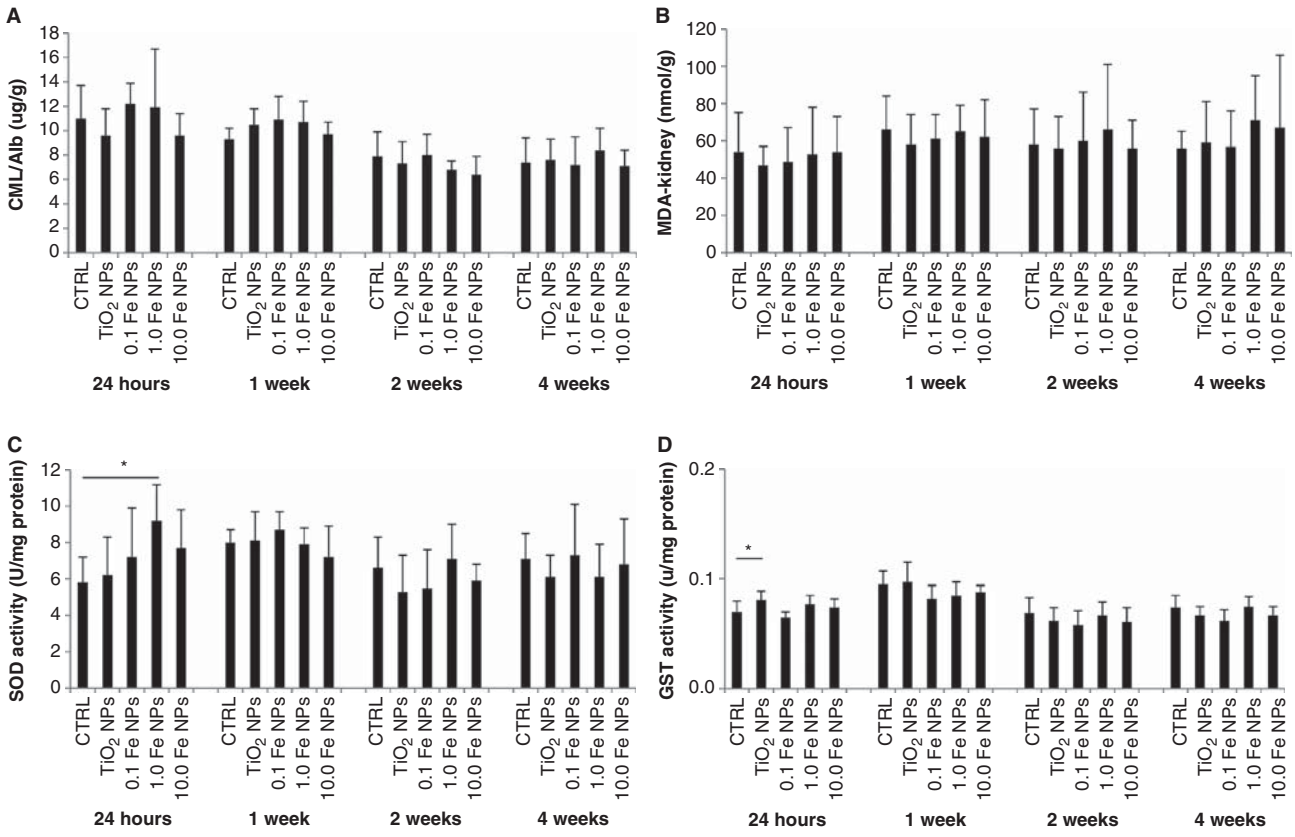

Figure 4. Levels of modified proteins and the activities of antioxidative enzymes in healthy rats after iv administration of single dose of NPs. (A) Plasma levels of N^{ε}-(carboxymethyl)lysine (CML, chemically derived AGE product, marker of glycoxidative reactions and a potential uremic toxin) corrected for albumin (Alb); (B) MDA content in the homogenates of renal cortex (expressed per 1 g of tissue) at sacrifice; (C) activity of superoxide dismutase (SOD) in renal cortex homogenates corrected for protein content; (D) activity of glutathione S-transferase (GST) in renal cortex homogenates corrected for protein content. Kruskal–Wallis test indicated significant difference among the groups at 24 h ($p = 0.021$). *Post hoc* comparisons of NP-administered groups with the controls were carried out using exact two-sided Mann–Whitney *U*-test with Bonferroni correction; $^*p < 0.05$; and (D) activity of GST in renal cortex homogenates corrected for protein content. Kruskal–Wallis test indicated significant difference among the groups at 24 h ($p = 0.004$). *Post hoc* analysis was performed as indicated above; $^*p < 0.05$; CTRL: placebo-administered rats; TiO_2 NPs: rats injected with iv bolus of TiO_2 NPs in dose of 1.0% of LD50; Fe NPs: oleate-coated USPIO NPs administered in doses corresponding to 0.1%, 1.0% and 10.0% of LD50, respectively. Rats were sacrificed 24 h, 1, 2 and 4 weeks after single administered dose. Each group represents mean (SD) from 6 to 8 animals.

no signs indicating an accumulation of iron NPs were revealed: under PAS staining no pigment deposition (i.e. iron) or siderophages were observed and both stainings for iron – either for Fe^{2+} and Fe^{3+} (Turnbull blue; Figure 5) or for Fe^{3+} only (Berlin Blue; data not shown) – remained negative. In Sirius red staining, a specific staining for collagen, all animals in all groups had a tubulointerstitial fibrosis score of 0, both in renal cortex and medulla (0–5% of cortex with fibrosis Figure 6). To exclude possible minor differences (below 5%), computer-based morphometry was used to quantify cortical and medullary collagen type I. Confirmatory to PAS and Sirius red staining, all groups showed a normal collagen type I expression, and no significant differences between the groups were observed (Figure 6). Glomeruli showed no collagen type I positivity (normal pattern).

General considerations

Seven rats died during the experiment: three rats did not recover from test-substance-administration-associated anaesthesia, one died during the blood pressure measurement, while three other rats deceased throughout the experiment, without clear relationship to particular NP administration, dosage or time interval after injection.

Administration of NPs did not elicit acute or postponed adverse effects on rat behaviour, fur appearance, and stool frequency, consistency or colour. Neither the mean food consumption (data not given), nor the mean daily weight gain or the body weight at sacrifice differed significantly among the treatment groups in corresponding time intervals (Supplementary Table Ia and Ib). Weight of the stools collected over 24 h from rats in metabolic cages showed no significant between-group difference (data not given). Systolic blood pressure did not differ significantly between groups sacrificed 4 weeks after administration of NPs (Supplementary Table Ib).

The animals sacrificed 4 weeks after administration of the highest dose of oleate-coated USPIO NPs displayed one to two enlarged (up to 3 mm) reddish-brown coloured para-iliac lymph nodes (predominantly those at the left side). Except for this finding, the macroscopic inspection did not reveal any accumulation of iron in other lymph nodes, or any organ (as would be inferred from change in colour). No visible lymph nodes- or organ-colour change, or overt pathology, was observed in the oleate-coated USPIO-administered animals sacrificed 24 h, 1 or 2 weeks after administration, and at any time interval in the animals exposed to TiO_2 NPs.

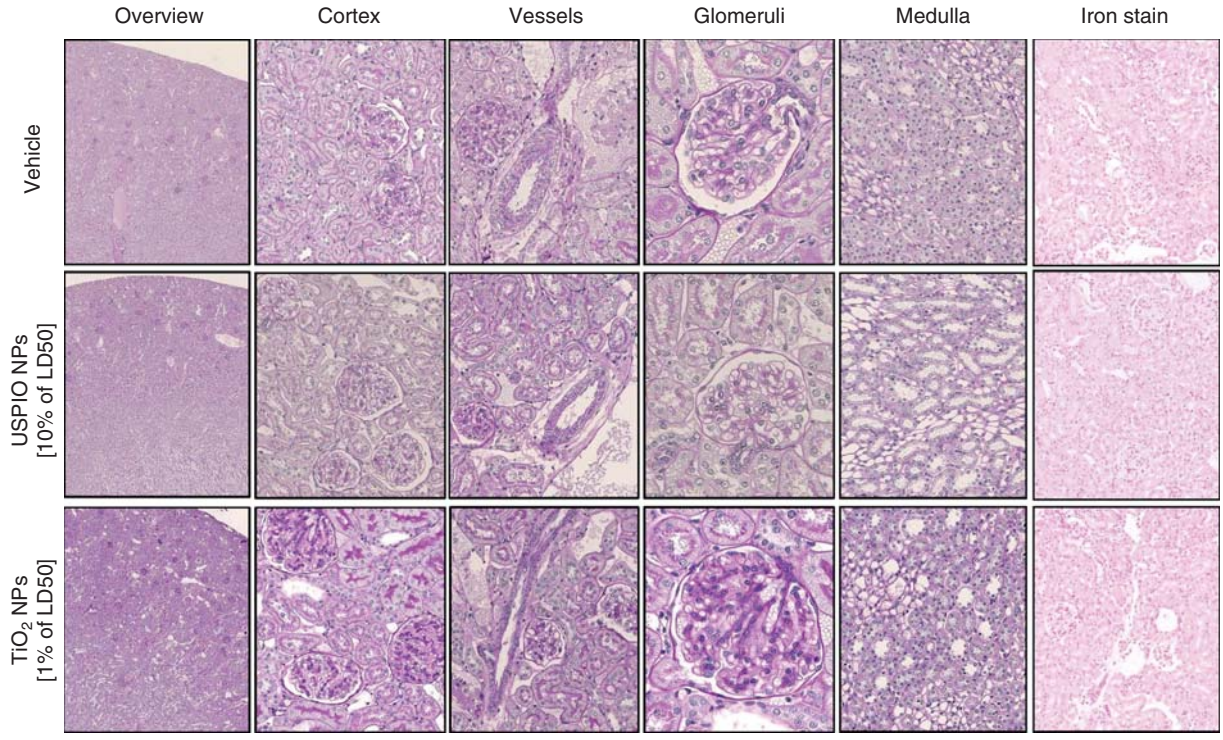

Figure 5. Renal histology in healthy rats after iv administration of single dose of NPs. Representative histology in rats 24 h after iv injection of vehicle (upper row), oleate-coated USPIO NPs in dose of 10% of LD50 (middle row) and Ti_2O nanoparticles in dose of 1% of LD50 (bottom row). No pathological changes were found either in cortical or medullary tubules, or in interstitium, glomeruli or vasculature. No iron deposition was observed in PAS or Turnbull blue stainings. Similar findings were observed in all other groups and time points. Pictures are shown in original magnifications: for overview 20×, for cortex, medulla and vessels 200×, for glomeruli 400× and for iron staining 100×.

Conventional toxicological parameters

At either time point the parameters of blood counts and plasma iron levels were within the normal range in all rats, and no significant between-group differences were revealed (Supplementary Table Ia and Ib).

No significant between-group differences in postprandial plasma glucose, insulin, cholesterol, triacylglycerol and bilirubin levels, or the activities of aspartate aminotransferase and alkaline phosphatase were observed in either time interval (Supplementary Table Ia and Ib). In comparison with the controls, at week 1 the rats administered oleate-coated USPIO NPs in dose of 1.0% and 10.0% of LD50 displayed mild transient elevation of plasma activities of alanine aminotransferase ($p < 0.0.5$), while plasma albumin levels differed significantly ($p = 0.05$), even though within the reference range, between the groups administered TiO_2 and oleate-coated USPIO NPs in a dose of 10.0% (Supplementary Table Ia).

Discussion

Owing to multiple functions of the kidney, to match the anticipated pattern of nephrotoxicity in *in vivo* studies, and to recognise the potential subclinical renal injury preceding a decline in renal function, a battery of tests should be combined. Employing complex methodological approach, after single iv injection (conditions of 100% bioavailability) we revealed no signs of acute or subacute nephrotoxicity of oleate-coated USPIO and TiO_2 NPs administered to healthy rats in dosages relevant to human exposure up to four weeks after administration.

Administration of TiO_2 and USPIO NPs – general findings

The Joint Scientific Committee for International Harmonization of Clinical Pathology Testing (Weingand et al. 1996) recommends to follow in organ/system-targeted toxicological studies also general morphologic pathology, core blood chemistry, haematology and histopathologic findings. These provide not only general information on the health status of the experimental animals, but may contribute to explanation of potential mechanisms of observed toxicity.

The single macroscopic sign of the administration of USPIO NPs was their accumulation in para-iliac lymph nodes in the animals sacrificed 4 weeks after single exposure to the highest applied dose, without significant alterations in plasma iron concentration. This is in line with the report on the fate of nanoparticular iron (ferumoxtran-10) administered *in vivo* in a dose of 2.6 mg Fe/kg: after initial vascular distribution, the particles are phagocytosed by the reticuloendothelial system, stored in lysosomes, ultimately entering the normal body iron metabolism (Islam & Wolf 2009). However, administration of high doses of nanoparticular iron leads to elevation of iron plasma levels, associated with the accumulation of nanoparticular iron in the liver and spleen, while the kidney iron content fluctuates only slightly to moderately above the background, suggesting that renal excretion of iron remains modest even after high load with iron NPs (Jain et al. 2008; Wang et al. 2010). Neither histopathological staining for Fe^{2+}/Fe^{3+} – a widely used diagnostic tool of iron deposition in pathology – nor as sensitive method as MRI confirmed enhanced iron accumulation within the kidney 24 h after single iv load with the highest dose of USPIO NPs (i.e. 3.64 mg

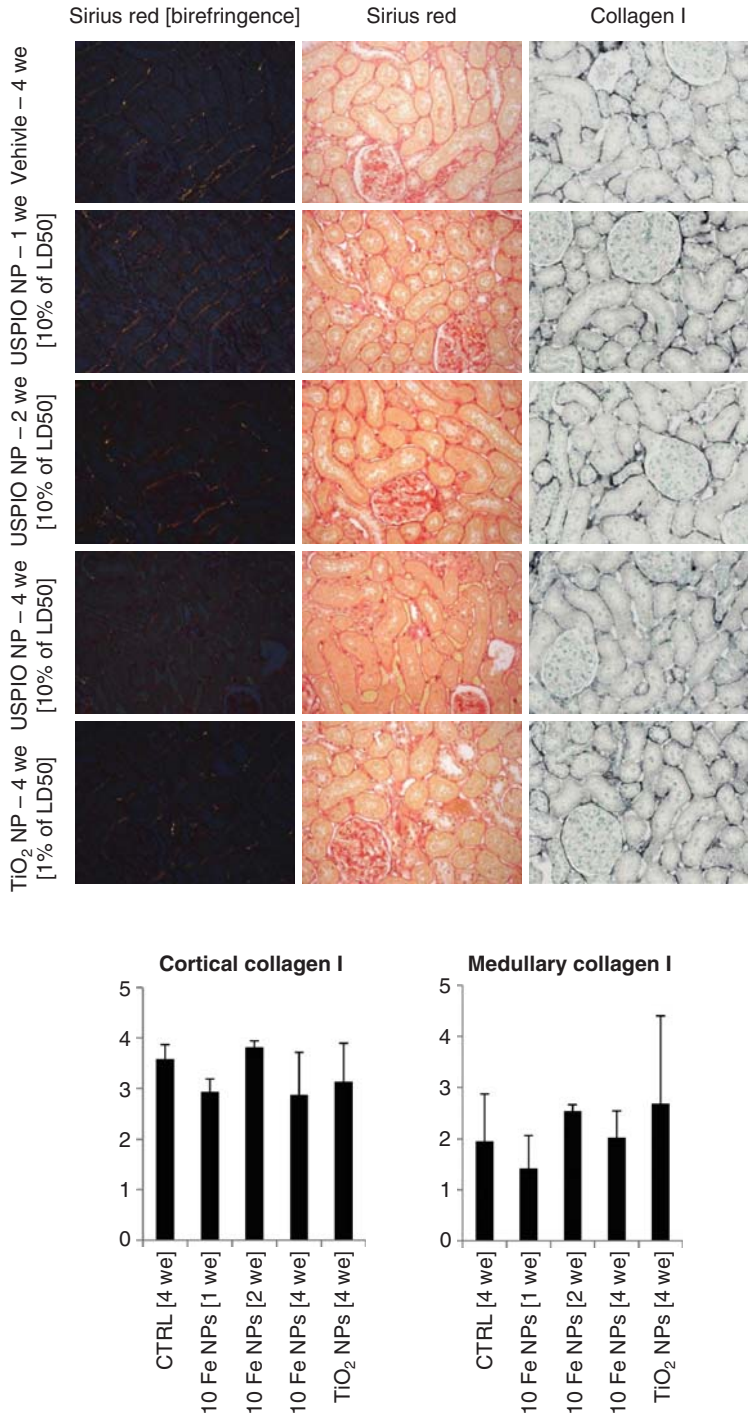

Figure 6. Assessment of renal fibrosis in healthy rats after iv administration of single dose of NPs. Representative slides of renal fibrosis in control animals after iv injection of vehicle (first row), oleate-coated USPIO NPs in dose of 10% of LD50 on week 1 (second row), week 2 (third row), week 4 (fourth row) and in TiO_2 NPs in dose of 1% of LD50 on week 4 (last row). No difference in renal fibrosis was observed using collagen-specific Sirius red staining (first column shows collagen specific birefringence in polarised light, the second column shows the same area in bright field). Quantification of collagen type I immunohistochemistry (using computer-based morphometry) confirmed these findings in both cortex and outer medulla (last column and both graphs). Data are means ± SD. Pictures are shown in original magnifications 200×.

Fe_3O_4/kg). The atomic absorption spectrometry study on biodistribution of Fe_3O_4 NPs administered in dose of 600 mg Fe_3O_4/kg (i.e. approximately 165-fold higher dose than that employed in our study) to mice revealed significant accumulation in kidneys, peaking at 6 h after administration, displaying still significant elevation (approximately by 43%, $p > 0.05$) at 24 h, but not in later time intervals (Wang et al. 2010). Thus, our data suggest that nanoparticular iron deposition within the kidneys 24 h after administration of USPIO NPs in a single dose of 3.64 mg Fe_3O_4/kg is minor and transitory, if any. However, in the meantime, MRI proved the accumulation of these particles in the livers of our animals, confirming that liver is a main target for deposition of USPIO NPs (Jain et al. 2008; Wang et al. 2010).

In the TiO_2 NP-administered rats no noticeable morphological changes or pathology were revealed. In the rats

exposed to iv injection of 10-fold higher dose of TiO_2 NPs than that applied in our study, the highest TiO_2 levels were revealed in liver, followed by spleen, and lung, peaking on day 1, but remaining high throughout the next 28 days (van Ravenzwaay et al. 2009). A minor increase on day 1 in TiO_2 levels in the kidney returned to control levels thereafter (van Ravenzwaay et al. 2009).

Evaluation of core hepatocellular (AST, ALT) and hepatobiliary markers (ALKP, bilirubin) did not reveal overt hepatotoxic effects: elevation in ALT activity at week 1 in rats administered the two higher dosages of oleate-coated USPIO NPs was too mild to be qualified as hepatocellular injury. Even if we hypothesise that the plasma liver enzyme activities peaked between days 1 and 7, they fully recovered later on. Magnitude of a transient early rise in AST, ALT and ALKP activities in rats administered iv nanoparticular iron in dose of 10 mg Fe/kg body weight reported in a different study did not represent abnormal liver function (Jain et al. 2008). A single iv administration of 10-fold higher dose of TiO_2 NPs than that used in our study did not elicit any pathology in blood chemistry parameters in rats within 28 days of the experiment (Fabian et al. 2008).

Administered NPs exerted clinically relevant impact neither on standard blood chemistry (glucose metabolism, lipid profile) nor hematologic parameters, which could aggravate potential nephrotoxicity. These data are in line with the report on administration of TiO_2 NPs (Fabian et al. 2008).

Nephrotoxicity

Renal function

In our study standard blood and urine tests of renal function did not reveal nephrotoxic effects of administered NPs. The rise in plasma sodium, calcium and magnesium, observed in our study 1 week after the administration of highest dose of oleate-coated USPIO NPs, was within the normal range of these parameters, and was neither associated with decreased renal excretion nor decreased fractional excretion of these elements. It could not be on the account of impurities present in applied oleate-coated USPIO NPs (Table I). As confirmed by determination of the renal excretion of KIM-1, the administered NPs did not elicit any injury to proximal tubules. KIM-1 – a type I transmembrane glycoprotein – is virtually undetectable in healthy kidney tissue, and abundantly up-regulated in injured proximal tubules (Ichimura et al. 1998; van Timmeren et al. 2007). Since the urinary KIM-1 is proportional to tissue KIM-1, it is widely used as a non-invasive biomarker of renal proximal tubular damage (Huo et al. 2010; van Timmeren et al. 2007). In the rats, iron overload, resulting in massive iron deposition-induced necrosis of proximal tubules, is associated with decline in renal function and plasma calcium, phosphate and potassium levels, and rise in the a activities of alkaline phosphatase and lactate dehydrogenase, reflecting combined impairment of renal function and bone mineral metabolism (Kudo et al. 2008). To our best knowledge, such alterations were not reported after administration of therapeutic/diagnostic dosages of either iv elemental, or nanoparticular iron. Thus, we suppose that the observed clinically insignificant elevation of plasma sodium, calcium and magnesium was artefactual. As mentioned above, iv administration of 10-fold higher dose of TiO_2 NPs did not elicit nephrotoxic effects in the former study (Fabian et al. 2008).

Effects of NPs on renal tissue

Rats subjected to passive smoking, or to intratracheal instillation of industrial dust amosite, develop glomerulosclerosis and tubulointerstitial fibrosis, associated with increased renal expression of collagen I, SOD and, partially, TGF-β_1 mRNA (Boor et al. 2009). These alterations on tissue and gene expression levels precede the clinical manifestation of kidney damage – thus, their presence is not yet accompanied by rise in plasma creatinine, urea and proteinuria or decline in creatinine clearance. To assure that administration of NPs is not accompanied by subclinical renal impairment, kidneys were subjected to histomorphologic and immunohistochemical evaluation, accompanied by gene expression studies, and assessment of oxidative status markers in renal cortex.

MDA, a naturally occurring by-product of polyunsaturated fatty acid peroxidation, is one of the most frequently used indicators of lipid peroxidation. Kidney MDA content rises with ageing (Shimizu et al. 2004), and to a much higher extent in course of chronic and acute renal failure (Kir et al. 2005; Mishra et al. 2008; Sebekova et al. 2001; Terrier-Lenglet et al. 2011), and in the latter cases not only due to recent lipid peroxidation, but also since protein-bound MDA fraction is not removed by kidneys (De Vecchi et al. 2009). Decreased renal-function-associated rise in kidney MDA content is accompanied by a decline in antioxidative enzyme activities (Padma et al. 2012). In the present study we revealed no clinically relevant rise in renal cortex MDA content after administration of NPs. However, four-fold higher iv load with nanoparticular iron elicited significant rise in renal tissue lipid hydroperoxides, which persisted over up to 7 days after administration, but they did not correlate with tissue iron accumulation (Jain et al. 2008). Despite that in our study tissue MDA content remained stable, we cannot unequivocally exclude transitorily enhanced local oxidative stress in kidneys of NP-administered rats. A rise in tissue antioxidant enzymes activities observed 24 h after administration of NPs might reflect the early and transient compensation of the imposed oxidative stress. Although we did not observe significant change in the total antioxidant capacity of renal cortex (estimated as ferric reducing ability of the tissue, a measure reflecting also non-enzymatic antioxidant systems), depletion of some single components of non-enzymatic antioxidative defense (such as glutathione, coenzyme Q, fat soluble vitamins) might not be excluded. However, even if the oxidative status of renal tissue had been temporarily disturbed, the challenge has not been translated into either overexpression of pro-fibrotic (TGF-β_1 and collagen I) or pro-inflammatory (TNF-α) genes in renal cortex, into altered renal histomorphology, or renal fibrosis.

Systemic oxidative stress and micro-inflammation

Iv-administered iron generates transitional oxidative stress, inflammation, endothelial dysfunction and renal injury (Agarwal et al. 2004; Bishu & Agarwal 2006; Lim & Vaziri

2004; Zager 2005). However, some of these alterations seem to peak earlier than the serum level of free iron, and not all iron compounds are equivalent in terms of their toxic effects. Thus, we focussed on biomarkers of oxidative damage and micro-inflammation potentially exerting nephrotoxic effects: advanced glycation end-products, AOPPs, protein carbonyls and MDA. These substances are formed spontaneously during ageing, and accumulate in tissues and body fluids (Brownlee 1995; Matsuyama et al. 2009; Shimizu et al. 2004; Witko-Sarsat et al. 1996). Their formation is markedly accelerated under different pathologic conditions (e.g. enhanced oxidative-, carbonyl- and/or nitrative stress, hyperglycaemia, oxidative burst of phagocytes) (Brownlee 1995; Matsuyama et al. 2009; Miyata et al. 2000; Witko-Sarsat et al. 1996). Moreover, they markedly accumulate in proportion to decline of renal function (Matsuyama et al. 2009; Schinzel et al. 2001; Šebeková et al. 2010; Witko-Sarsat et al. 1996). However, they are not innocent bystanders: AGEs alter the structure and function of proteins, and their interaction with a specific cell-surface receptor RAGE (receptor for AGEs) may lead to production of reactive oxygen species, pro-atherogenic and pro-inflammatory events, resulting, among others, in renal fibrosis (Bierhaus et al. 2005; Thomas 2011; Thornalley & Rabbani 2009). Lipid peroxidation and formation of protein carbonyls in kidney tissue alter the structure and function of cellular and matrix proteins contributing to the onset of kidney lesions (Miyata et al. 2000; Poirier et al. 2000). Herein we determined AGE-associated fluorescence of plasma as a bulk estimate of the formation of AGE products with intrinsic fluorescence, as well as a chemically defined non-fluorescent AGE product of glycoxidation reactions – N^{ε}-(carboxymethyl)lysine; plasma MDA and protein carbonyl levels. Neither of these markers was affected significantly after administration of NPs, supporting the conclusion that even if the administered NPs temporarily altered the oxidative status, this was not translated into enhanced oxidative and carbonyl stress, which could contribute to induction of a decline in renal function.

AOPPs – formed *in vivo* mainly via myeloperoxidase reaction by chlorinated oxidants – hypochloric acid and chloramines – are considered as pro-inflammatory mediators that can damage biological membranes and impair HDL-cholesterol metabolism (Marsche et al. 2009) and elicit endothelial dysfunction via reducing endothelium-derived NO synthesis and trigging reactive oxygen species production in a RAGE-dependent manner (Guo et al. 2008; Chen et al. 2008), and their accumulation promotes renal fibrosis and deteriorates renal function, probably via a redox-sensitive inflammatory pathway (Li et al. 2007). AOPPs represent oxidatively modified proteins serving also as markers of activation of neutrophils of phagocytes (Witko-Sarsat et al. 1996). Administration of NPs did not affect AOPP levels significantly. Together with the data on white blood cell counts, and hsCRP, these findings indicate that iv application of NPs did not elicit overt systemic inflammatory reaction or micro-inflammation. Absence of the induction of the expression of pro-inflammatory tumour necrosis factor-α gene in renal cortex, with concurrent negative findings regarding the infiltration of kidney tissue by inflammatory cells, suggests that systemic administration of the NPs did not elicit local inflammation in the kidneys.

ADMA is one of the most potent endogenous inhibitors of NO synthase, and elevated ADMA levels are associated with major cardiovascular events and total mortality in diverse patient populations (Boger 2005; Fliser 2005). While in chronic renal insufficiency, plasma levels of ADMA increase due to loss of excretory function of the kidney, during short-term acute renal failure ADMA is metabolised into citrulline and dimethylamine by dimethylarginine dimethylaminohydrolase, resulting in a decline in circulating levels of ADMA (Carello et al. 2006). In our rats the levels of ADMA remained steady after administration of NPs, supporting the assumption that administration of NPs was not associated with either transitory acute or slowly developing mild chronic renal insufficiency. Moreover, we might anticipate that administration of NPs does not impose negative effects on endothelial vasodilation, at least via the above-mentioned mechanism.

Our data showing that iv administration of TiO_2 NPs does not evoke systemic oxidative stress or micro-inflammation are in line with those of Fabian et al. (Fabian et al. 2008), reporting that wide range of pro-inflammatory markers and cytokines remains unaffected by iv TiO_2 NPs. The absence of inflammatory response should be interpreted with caution because of interspecies differences in human and animal inflammatory/immune response (Bailey et al. 2012; Mestas & Hughes 2004). Clarification of this question requires aimed studies focussing on immunomodulatory potential of nanomaterials (De Jong & Van Loveren 2007; Pfaller et al. 2010).

Former studies on the toxicity of iv-administered metallic NPs did not focus primarily on nephrotoxicity, tested NPs with different properties than those in our study, and doses higher than relevant for humans. However, in line with our data, standard blood chemistry and renal histology did not reveal nephrotoxicity after single iv administration of either USPIO (size: 11 ± 2 nm, 10 mg iron/kg body weight) or TiO_2 NPs (size: 20–30 and 200 nm, 5 mg/kg) to rats in acute and subchronic studies (Fabian et al. 2008; Jain et al. 2008; van Ravenzwaay et al. 2009). On the other hand, metabonomic analyses of body fluids and organ-specific responses to iv-administered USPIO NPs (size: 10 ± 2 nm and 20 ± 2 nm) in a single dose to rats in acute setting revealed transient changes that might be attributed to the disturbance of renal function (Feng et al. 2010; Feng et al. 2011). It remains unclear whether these responses followed the administration of clinically relevant dose, since the amount of administered iron was not specified precisely.

Limitations

Like in the vast majority of the papers dealing with P25, the exact crystalline composition of TiO_2 NPs used in our study remains unclear (Ohtani et al. 2010). The supplier (Degussa, Evonik) does not report the exact crystalline composition of P25. In contrast to USPIO, titanium NPs are not paramagnetic; thus, it was not possible to follow their potential accumulation in the kidneys. Young female rats were used

in this study. However, neither reference values for renal function parameters (except those affected by extrarenal factors, such as plasma creatinine concentration), nor histomorphology of healthy kidney differ between males and females. Rats were not synchronised for estral cycle. In the rats GFR shows no significant difference in proestrus and diestrus (Santmyire et al. 2010). We are not aware of any report on menstrual/estral cycle-dependent changes in proteinuria, or plasma levels and renal excretion of other elements or molecules investigated by us, renal histology, or renal expression of pro-fibrotic or pro-inflammatory genes, including their transcription into the proteins. Neither the general recommendations for toxicological studies in experimental animals (Weingand et al. 1996) nor the OECD guidelines state that in case of females the estral-cycle-synchronised animals should be used in experimental studies on nephrotoxicity. Our results are pertinent to effects obtained in young healthy rats up to 4 weeks after administration, and can be extrapolated to administration of NPs neither to elderly animals, nor to those with comorbidities. Extrapolation of our experimental data on general toxicity and nephrotoxicity of studied NPs into recommendation on safe use in clinical application might be limited by the different immune system functions between rats and humans (Bailey et al. 2012; Crawford et al. 1994; Mestas & Hughes 2004; Van Loveren et al. 1998).

Conclusion

Herein we present for a first time comprehensive experimental data on the nephrotoxicity of two different types of metallic NPs under conditions of 100% bioavailability, in dosages relevant to human exposure. The effects of oleate-coated USPIO NPs were tested in a wide concentration range. Simultaneous analyses of standard and special blood and urine parameters of renal function and multitude investigations of renal tissue suggest that administered NPs neither cause nephrotoxic effects nor induce inflammation or oxidative stress. No signs of haemato- or hepato-toxicity were revealed. Data obtained by multifaceted approach enable the prediction of human nephrotoxicity during preclinical studies, and may serve as comparison for alternative testing strategies using *in vitro and in silico* methods essential for the NP-nephrotoxicity risk assessment.

Acknowledgement

This study was supported by 7FP EC grant to NanoTest project, contract No. HEALTH-2007-201335, and in part by grants from Ministry of Education of Slovak Republic, No. VEGA 2/0149/12, and the Deutsche Forschungsgemeinschaft (to PB: BO 3755/1-1 and SFB TRR57, projects nP25 and Q1). Authors wish to thank MVDr. Katarína Ambrušová, the Head of the Animal Facility at Slovak Medical University in Bratislava, for excellent assistance throughout the experiment; Dipl. Tex. Des. Zuzana Šebeková from the Academy of Fine Arts and Design, Bratislava, for excellent technical assistance at sacrifice, and RNDr. Vladimír Mlynárik from Laboratory of Functional and Metabolic Imaging, Ecole Polytechnique Fédérale de Lausanne, Lausanne, Switzerland, for his valuable advices and comments regarding MRI data processing.

Declaration of interest

The authors report no conflicts of interest. The authors alone are responsible for the content and writing of the paper.

References

Agarwal R, Vasavada N, Sachs NG, Chase S. 2004. Oxidative stress and renal injury with intravenous iron in patients with chronic kidney disease. Kidney Int 65:2279–2289.

Aurelie NDC, Touyz RM. 2011. A new look at the renin-angiotensin system-focusing on the vascular system. Peptides 32:2141–2150.

Bailey M, Christoforidou Z, Lewis MC. 2012. The evolutionary basis for differences between the immune systems of man, mouse, pig and ruminants. Vet Immunol Immunopathol http://dx.doi.org/10.1016/j.vetimm.2012.09.022.

Benzie IF, Strain JJ. 1996. The ferric reducing ability of plasma (FRAP) as a measure of "antioxidant power": the FRAP assay. Anal Biochem 239:70–76.

Bierhaus A, Humpert PM, Morcos M, Wendt T, Chavakis T, Arnold B, et al. 2005. Understanding RAGE, the receptor for advanced glycation end products. J Mol Med (Berl) 83:876–886.

Bishu K, Agarwal R. 2006. Acute injury with intravenous iron and concerns regarding long-term safety. Clin J Am Soc Nephrol 1(Suppl 1):S19–S23.

Boger RH. 2005. Asymmetric dimethylarginine (ADMA) and cardiovascular disease: insights from prospective clinical trials. Vasc Med 10(Suppl 1):S19–S25.

Boor P, Casper S, Celec P, Hurbankova M, Beno M, Heidland A, et al. 2009. Renal, vascular and cardiac fibrosis in rats exposed to passive smoking and industrial dust fibre amosite. J Cell Mol Med 13:4484–4491.

Boor P, Konieczny A, Villa L, Kunter U, van Roeyen CR, LaRochelle WJ, et al. 2007. PDGF-D inhibition by CR002 ameliorates tubulointerstitial fibrosis following experimental glomerulonephritis. Nephrol Dial Transplant 22:1323–1331.

Boor P, Celec P, Martin IV, Villa L, Hodosy J, Klenovicsová K, et al. 2011. The peroxisome proliferator-activated receptor-alpha agonist, BAY PP1, attenuates renal fibrosis in rats. Kidney Int 80:1182–1197.

Bradford MM. 1976. A rapid and sensitive method for the quantitation of microgram quantities of protein utilizing the principle of protein-dye binding. Anal Biochem 72:248–254.

Brownlee M. 1995. Advanced protein glycosylation in diabetes and aging. Annu Rev Med 46:223–234.

Carello KA, Whitesall SE, Lloyd MC, Billecke SS, D'Alecy LG. 2006. Asymmetrical dimethylarginine plasma clearance persists after acute total nephrectomy in rats. Am J Physiol Heart Circ Physiol 290:H209–H216.

Cavarocchi NC, England MD, O'Brien JF, Solis E, Russo P, Schaff HV, et al. 1986. Superoxide generation during cardiopulmonary bypass: is there a role for vitamin E? J Surg Res 40:519–527.

Celec P, Hodosy J, Behuliak M, Palffy R, Gardlik R, Halcak L, et al. 2012. Oxidative and carbonyl stress in patients with obstructive sleep apnea treated with continuous positive airway pressure. Sleep Breath 16:393–398.

Chen SX, Song T, Zhou SH, Liu YH, Wu SJ, Liu LY. 2008. Protective effects of ACE inhibitors on vascular endothelial dysfunction induced by exogenous advanced oxidation protein products in rats. Eur J Pharmacol 584:368–375.

Crawford RM, Leiby DA, Green SJ, Nacy CA, Fortier AH, Meltzer MS. 1994. Macrophage activation: a riddle of immunological resistance. Immunol Ser 60:29–46.

Cruz DN, Fard A, Clementi A, Ronco C, Maisel A. 2012. Role of biomarkers in the diagnosis and management of cardio-renal syndromes. Semin Nephrol 32:79–92.

De Jong WH, Van Loveren H. 2007. Screening of xenobiotics for direct immunotoxicity in an animal study. Methods 41:3–8.

De Vecchi AF, Bamonti F, Novembrino C, Ippolito S, Guerra L, Lonati S, et al. 2009. Free and total plasma malondialdehyde in chronic renal insufficiency and in dialysis patients. Nephrol Dial Transplant 24:2524–2529.

Duguet E, Vasseur S, Mornet S, Devoisselle JM. 2006. Magnetic nanoparticles and their applications in medicine. Nanomedicine 1:157–168.

Dusinska M, Fjellsbø L, Magdolenova Z, Rinna A, Runden Pran E, Bartonova A, et al. 2009. Testing strategies for the safety of nanoparticles used in medical applications. Nanomedicine (Lond) 4:605–607.

Fabian E, Landsiedel R, Ma-Hock L, Wiench K, Wohlleben W, van Ravenzwaay B. 2008. Tissue distribution and toxicity of intravenously administered titanium dioxide nanoparticles in rats. Arch Toxicol 82:151–157.

Fadda LM, Abdel Baky NA, Al-Rasheed NM, Al-Rasheed NM, Fatani AJ, Atteya M. 2012. Role of quercetin and arginine in ameliorating nano zinc oxide-induced nephrotoxicity in rats. BCM Complement Altern Med 12:60e.

Feng J, Liu H, Zhang L, Bhakoo K, Lu L. 2010. An insight into the metabolic responses of ultra-small superparamagnetic particles of iron oxide using metabonomic analysis of biofluids. Nanotechnology 21:395101.

Feng J, Liu H, Bhakoo KK, Lu L, Chen Z. 2011. A metabonomic analysis of organ specific response to USPIO administration. Biomaterials 32:6558–6569.

Fliser D. 2005. Asymmetric dimethylarginine (ADMA): the silent transition from an 'uraemic toxin' to a global cardiovascular risk molecule. Eur J Clin Invest 35:71–79.

Guo ZJ, Niu HX, Hou FF, Zhang L, Fu N, Nagai R, et al. 2008. Advanced oxidation protein products activate vascular endothelial cells via a RAGE-mediated signaling pathway. Antioxid Redox Signal 10:1699–1712.

Habig WH, Pabst MJ, Jakoby WB. 1974. Glutathione S-transferases. The first enzymatic step in mercapturic acid formation. J Biol Chem 249:7130–7139.

Han WK, Bailly V, Abichandani R, Thadhani R, Bonventre JV. 2002. Kidney Injury Molecule-1 (KIM-1): a novel biomarker for human renal proximal tubule injury. Kidney Int 62:237–244.

Holsapple MP, Farland WH, Landry TD, Monteiro-Riviere NA, Carter JM, Walker NJ, et al. 2005. Research strategies for safety evaluation of nanomaterials, part II: Toxicological and safety evaluation of nanomaterials, current challenges and data needs. Toxicol Sci 88:12–17.

Huo W, Zhang K, Nie Z, Li Q, Jin F. 2010. Kidney injury molecule-1 (KIM-1): a novel kidney-specific injury molecule playing potential double-edged functions in kidney injury. Transplant Rev (Orlando) 24:143–146.

Ichimura T, Bonventre JV, Bailly V, Wei H, Hession CA, Cate RL, et al. 1998. Kidney injury molecule-1 (KIM-1), a putative epithelial cell adhesion molecule containing a novel immunoglobulin domain, is up-regulated in renal cells after injury. J Biol Chem 273:4135–4142.

Islam T, Wolf G. 2009. The pharmacokinetics of the lymphotropic nanoparticle MRI contrast agent ferumoxtran-10. Cancer Biomark 5:69–73.

Ismagilov ZR, Tsykoza LT, Shikina NV, Zarytova VF, Zinoviev VV, Zagrebelnyi SN. 2009. Synthesis and stabilization of nano-sized titanium dioxide. Russian Chem Rev 78:873–885.

Jain TK, Reddy MK, Morales MA, Leslie-Pelecky DL, Labhasetwar V. 2008. Biodistribution, clearance, and biocompatibility of iron oxide magnetic nanoparticles in rats. Mol Pharm 5:316–327.

Kenzaoui BH, Bernasconi CC, Guney-Ayra S, Juillerat-Jeanneret L. 2012. Induction of oxidative stress, lysosome activation and autophagy by nanoparticles in human brain-derived endothelial cells. Biochem J 441:813–821.

Kim JE, Shin JY, Cho MH. 2012. Magnetic nanoparticles: an update of application for drug delivery and possible toxic effects. Arch Toxicol 86:685–700.

Kir HM, Dillioglugil MO, Tugay M, Eraldemir C, Ozdogan HK. 2005. Effects of vitamins E, A and D on MDA, GSH, NO levels and SOD activities in 5/6 nephrectomized rats. Am J Nephrol 25:441–446.

Koomans HA, Blankestijn PJ, Joles JA. 2004. Sympathetic hyperactivity in chronic renal failure: a wake-up call. J Am Soc Nephrol 15:524–537.

Koska J, Syrova D, Blazicek P, Marko M, Grna JD, Kvetnansky R, et al. 1999. Malondialdehyde, lipofuscin and activity of antioxidant enzymes during physical exercise in patients with essential hypertension. J Hypertens 17:529–535.

Kudo H, Suzuki S, Watanabe A, Kikuchi H, Sassa S, Sakamoto S. 2008. Effects of colloidal iron overload on renal and hepatic siderosis and the femur in male rats. Toxicology 246:143–147.

Laniado M, Chachuat A. 1995. The endorem tolerance profile. Radiologe 35:S266–S270.

Lei RH, Wu CQ, Yang BH, Ma HZ, Shi C, Wang QJ, et al. 2008. Integrated metabolomic analysis of the nano-sized copper particle-induced hepatotoxicity and nephrotoxicity in rats: a rapid in vivo screening method for nanotoxicity. Toxicol Appl Pharmacol 232:292–301.

Li HY, Hou FF, Zhang X, Chen PY, Liu SX, Feng JX, et al. 2007. Advanced oxidation protein products accelerate renal fibrosis in a remnant kidney model. J Am Soc Nephrol 18:528–538.

Liao MY, Liu HG. 2012. Gene expression profiling of nephrotoxicity from copper nanoparticles in rats after repeated oral administration. Environ Toxicol Pharmacol 34:67–80.

Lim CS, Vaziri ND. 2004. Iron and oxidative stress in renal insufficiency. Am J Nephrol 24:569–575.

Magdolenova Z, Rinna A, Fjellsbo L, Dusinska M. 2011. Safety assessment of nanoparticles cytotoxicity and genotoxicity of metal manoparticles in vitro. J Biomed Nanotechnol 7:20–21.

Majewski P, Thierry B. 2007. Functionalized magnetite nanoparticles - synthesis, properties, and bio-applications. Crit Rev Solid State Mater Sci 32:203–215.

Marsche G, Frank S, Hrzenjak A, Holzer M, Dirnberger S, Wadsack C, et al. 2009. Plasma-advanced oxidation protein products are potent high-density lipoprotein receptor antagonists in vivo. Circ Res 104:750–757.

Matsuyama Y, Terawaki H, Terada T, Era S. 2009. Albumin thiol oxidation and serum protein carbonyl formation are progressively enhanced with advancing stages of chronic kidney disease. Clin Exp Nephrol 13:308–315.

Mestas J, Hughes CCW. 2004. Of mice and not men: differences between mouse and human immunology. J Immunol 172:2731–2738.

Mishra OP, Pooniya V, Ali Z, Upadhyay RS, Prasad R. 2008. Antioxidant status of children with acute renal failure. Pediatr Nephrol 23:2047–2051.

Miyata T, Kurokawa K, van Ypersele de Strihou C. 2000. Relevance of oxidative and carbonyl stress to long-term uremic complications. Kidney Int Suppl 76:S120–S125.

Munch G, Keis R, Wessels A, Riederer P, Bahner U, Heidland A, et al. 1997. Determination of advanced glycation end products in serum by fluorescence spectroscopy and competitive ELISA. Eur J Clin Chem Clin Biochem 35:669–677.

Oberdorster G. 2010. Safety assessment for nanotechnology and nanomedicine: concepts of nanotoxicology. J Intern Med 267:89–105.

OECD. 2000. Guidance Document on Acute Oral Toxicity. Environmental Health and Safety Monograph Series on Testing and Assessment No. 24.

Ohtani B, Prieto-Mahaney OO, Li D, Abe R. 2010. What is Degussa (Evonik) P25? Crystalline composition analysis, reconstruction from isolated pure particles and photocatalytic activity test. J Photochem Photobiol A-Chem 216:179–182.

Padma VV, Baskaran R, Roopesh RS, Poornima P. 2012. Quercetin attenuates lindane induced oxidative stress in wistar rats. Mol Biol Rep 39:6895–6905.

Paglia DE, Valentine WN. 1967. Studies on the quantitative and qualitative characterization of erythrocyte glutathione peroxidase. J Lab Clin Med 70:158–169.

Pándics T. 2008. Clinical application of nanoparticles, and their possible health risk. Orv Hetil 149:1785–1790.

Park JH, Kim S, Bard AJ. 2006. Novel carbon-doped TiO2 nanotube arrays with high aspect ratios for efficient solar water splitting. Nano Lett 6:24–28.

Pfaller T, Colognato R, Nelissen I, Favilli F, Casals E, Ooms D, et al. 2010. The suitability of different cellular in vitro immunotoxicity and genotoxicity methods for the analysis of nanoparticle-induced events. Nanotoxicology 4:52–72.

Poirier B, Lannaud-Bournoville M, Conti M, Bazin R, Michel O, Bariety J, et al. 2000. Oxidative stress occurs in absence of hyperglycaemia and inflammation in the onset of kidney lesions in normotensive obese rats. Nephrol Dial Transplant 15:467–476.

Pujalte I, Passagne I, Brouillaud B, Treguer M, Durand E, Ohayon-Courtes C, et al. 2011. Cytotoxicity and oxidative stress induced by different metallic nanoparticles on human kidney cells. Part Fibre Toxicol 8:10.

Rosner MH, Ronco C, Okusa MD. 2012. The role of inflammation in the cardio-renal syndrome: a focus on cytokines and inflammatory mediators. Semin Nephrol 32:70–78.

Santmyire BR, Venkat V, Beinder E, Baylis C. 2010. Impact of the estrus cycle and reduction in estrogen levels with aromatase inhibition, on renal function and nitric oxide activity in female rats. Steroids 75:1011–1015.
Sebekova K, Blazicek P, Syrova D, Krivosikova Z, Spustova V, Heidland A, et al. 2001. Circulating advanced glycation end product levels in rats rapidly increase with acute renal failure. Kidney Int Suppl 78:S58–S62.
Shimizu MH, Araujo M, Borges SM, de Tolosa EM, Seguro AC. 2004. Influence of age and vitamin E on post-ischemic acute renal failure. Exp Gerontol 39:825–830.
Schinzel R, Munch G, Heidland A, Sebekova K. 2001. Advanced glycation end products in end-stage renal disease and their removal. Nephron 87:295–303.
Singbartl K. 2011. Renal-pulmonary crosstalk. In: Kellum JA, Ronco C, Vincent JL, editors. Controversies in acute kidney injury. Basel: Karger. Vol. 174. pp 65–70.
Star RA. 1998. Treatment of acute renal failure. Kidney Int 54:1817–1831.
Stern ST, McNeil SE. 2008. Nanotechnology safety concerns revisited. Toxicol Sci 101:4–21.
Sun J, Zhou S, Hou P, Yang Y, Weng J, Li X, et al. 2007. Synthesis and characterization of biocompatible Fe3O4 nanoparticles. J Biomed Mater Res A 80:333–341.
Šebeková K Jr, Blažíc̆ek P, Syrová D, Galbavý Š, Schinzel R, Heidland A, et al. 2010. Oxidative stress, advanced glycation end products and residual renal function in the rat model of unilateral ureteral obstruction: effects of phlogenzym and losartan. Biopolymers Cell 26:121–127.
Terrier-Lenglet A, Nollet A, Liabeuf S, Barreto DV, Brazier M, Lemke HD, et al. 2011. Plasma malondialdehyde may not predict mortality in patient with chronic kidney disease. Nephrol Ther 7:219–224.
Tetley TD. 2007. Health effects of nanomaterials. Biochem Soc Trans 35:527–531.
Thomas MC. 2011. Advanced glycation end products. In: Lai KN, Tang SCW, editors. Diabetes and the kidney. Vol. 170. pp 66–74.
Thornalley PJ, Rabbani N. 2009. Highlights and hotspots of protein glycation in end-stage renal disease. Semin Dial 22:400–404.
Vaidya VS, Ozer JS, Dieterle F, Collings FB, Ramirez V, Troth S, et al. 2010. Kidney injury molecule-1 outperforms traditional biomarkers of kidney injury in preclinical biomarker qualification studies. Nat Biotechnol 28:478–485.
Van Loveren H, De Jong WH, Vandebriel RJ, Vos JG, Garssen J. 1998. Risk assessment and immunotoxicology. Toxicol Lett 103:261–265.
van Ravenzwaay B, Landsiedel R, Fabian E, Burkhardt S, Strauss V, Ma-Hock L. 2009. Comparing fate and effects of three particles of different surface properties: nano-TiO(2), pigmentary TiO(2) and quartz. Toxicol Lett 186:152–159.
van Timmeren MM, van den Heuvel MC, Bailly V, Bakker SJ, van Goor H, Stegeman CA. 2007. Tubular kidney injury molecule-1 (KIM-1) in human renal disease. J Pathol 212:209–217.
Vanholder R, De Smet R, Glorieux G, Argilés A, Baurmeister U, Brunet P, et al. 2003. Review on uremic toxins: classification, concentration, and interindividual variability. Kidney Int 63:1934–1943.
Volkovova K, Beno M, Tulinska J, Handy R, Dusinska M. 2013. Median lethal dose of titanium dioxide and Na-oleate coated iron oxide nanoparticles after single intravenous injection to adult rats. Acute toxicity study. Nanotoxicology; in press.
Wang J, Chen Y, Chen B, Ding J, Xia G, Gao C, et al. 2010. Pharmacokinetic parameters and tissue distribution of magnetic Fe(3)O(4) nanoparticles in mice. Int J Nanomedicine 5:861–866.
Wang JX, Zhou G, Chen C, Yu H, Wang T, Ma Y, et al. 2007. Acute toxicity and biodistribution of different sized titanium dioxide particles in mice after oral administration. Toxicol Lett 168:176–185.
Weingand K, Brown G, Hall R, Davies D, Gossett K, Neptun D, et al. 1996. Harmonization of animal clinical pathology testing in toxicity and safety studies. Fundam Appl Toxicol 29:198–201.
Witko-Sarsat V, Friedlander M, Capeillere-Blandin C, Nguyen-Khoa T, Nguyen AT, Zingraff J, et al. 1996. Advanced oxidation protein products as a novel marker of oxidative stress in uremia. Kidney Int 49:1304–1313.
Wong SH, Knight JA, Hopfer SM, Zaharia O, Leach CN Jr, Sunderman FW Jr. 1987. Lipoperoxides in plasma as measured by liquid-chromatographic separation of malondialdehyde-thiobarbituric acid adduct. Clin Chem 33:214–220.
Yan GY, Huang Y, Bu Q, Lv L, Deng P, Zhou J, et al. 2012. Zinc oxide nanoparticles cause nephrotoxicity and kidney metabolism alterations in rats. J Environ Sci Health A Tox Hazard Subst Environ Eng 47:577–588.
Zager RA. 2005. Parenteral iron treatment induces MCP-1 accumulation in plasma, normal kidneys, and in experimental nephropathy. Kidney Int 68:1533–1542.
Zhang R, Niu YJ, Li YW, Zhao CF, Song B, Li Y, et al. 2010. Acute toxicity study of the interaction between titanium dioxide nanoparticles and lead acetate in mice. Environ Toxicol Pharmacol 30:52–60.

Supplementary material available online

Supplementary Tables I–III.